09 Aug 2017

Effect of Optimizing Particle Size in Laser Metal Deposition with Blown Pre-Mixed Powders

Wei Li

Jingwei Zhang

Xinchang Zhang

Sreekar Karnati

et. al. For a complete list of authors, see https://scholarsmine.mst.edu/mec_aereng_facwork/4385

Recommended Citation

EFFECT OF OPTIMIZING PARTICLE SIZE IN LASER METAL DEPOSITION WITH BLOWN

PRE-MIXED POWDERS

W. Li[a], J. W. Zhang[a], X. C. Zhang[a], S. Karnati[a], F. Liou[a].

[a]Department of Mechanical and Aerospace Engineering, Missouri University of Science and Technology, Rolla, MO 65409, United States

Abstract

Functionally Graded Material (FGM) is often fabricated by Laser metal deposition with pre-mixed multiple powders (PMM-powder). Since the supplied PMM-powder directly affects FGM's composition, investigation on PMM-powder's property is greatly needed. This paper employed experimental method to observe an important problem: PMM-powder separation in fabricating FGM. A novel particle size optimization method was introduced as solution to eliminate the powder separation. Pre-mixed pure Cu and 4047 Al powders were used to do two experiments. The first experiment result disclosed the existence of powder separation. By optimizing the particle size, the PMM-powder separation was effectively solved in the second experiment result.

Keywords: Functionally Gradient Material; Pre-Mixed Multi-Powder; Laser metal deposition; powder separation; composition deviation.

1. Introduction

Functionally Gradient Material (FGM) is arousing more and more attention in area of advanced material processing. Gradual variation in composition and structure over volume in FGM [1], result in corresponding gradual changes in the properties of the material to meet the usage requirements. FGM can be designed for specific functions and applications, and can combine two or more different materials into one structure and perform multiple functions [2, 3]. To fabricate the FGM structure, laser metal deposition is an effective process technique, in which gradually varying in composition over volume is achieved by Pre-Mixed Multi-Powder (PMM-powder) [4, 5]. Fig.1 is schematic illustration of fabricating FGM by laser metal deposition.
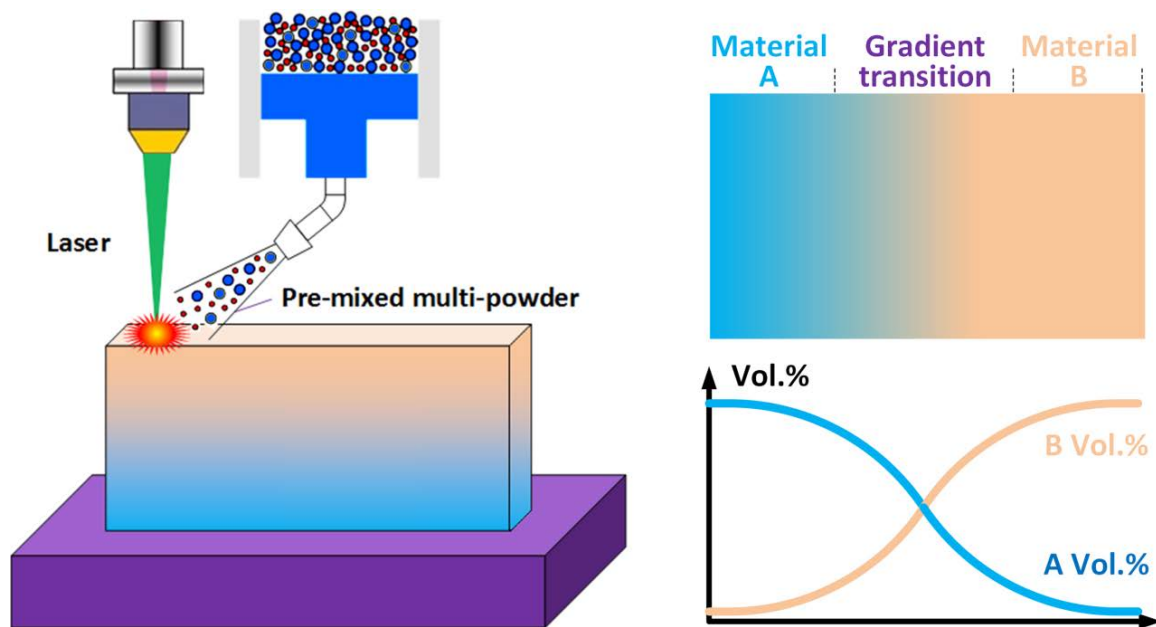
Fig.1. Schematic illustration of fabricating FGM by Laser metal deposition.

A necessary factor in FGM fabrication is the multi-composition powder, which is often pre-mixed of two kinds of alloy or metal elemental powders according to the composition requirement of FGM structure. In the process of Laser metal deposition, the PMM-powder are input into powder feeder. Inert argon gas flow drives the powders to move along the powder feeder pipe. Since the PMM-powders have different particle densities and sizes, under the same argon gas flow, light and small particles could move faster while heavy and big particles could lag behind. This kind of particle flow dynamics may cause powder separation and composition deviation in PMM-powder. In FGM structure, the material composition ratio in any different area is required strictly (Fig.1). Non-uniform PMM-powders will ruin the gradually varying material composition ratio, and further discount the wanted material performance. Therefore, to address this issue, investigation on PMM-powder during laser metal deposition is greatly needed. So far, there is no special study focusing on pre-mixed multiple powders' dynamic behavior in fabricating FGM by laser metal deposition. Some previous research results about the powder flow were just for identical material through both numerical and experimental methods [6-10].

In this paper, experimental method was employed to observe powder separation in fabricating FGM with blown PMM-powders. A novel particle size optimization method was introduced as solution to eliminate the powder separation. Pre-mixed pure Cu and 4047 Al powders were used to do two experiments. The first experiment result disclosed the existence of powder separation. By optimizing the particle size in two types of powder, the powder separation was effectively solved in the second experiment result.

2. Experiment procedure

2.1. Experiment set-up

The experiment set-up is schematically shown in Fig.2. A commercial powder feeder (Bay State Surface Technologies, Inc, Model-1200) was used to supply PMM-powder. Pure Cu powder and 4047 Al powder (Fig.2) were used in the experiments. The particles size distributions were displayed by the sieve analysis in Table.1 and Table.2. A plastic pipe, with 1.5 m in length and 5 mm in inner diameter, delivers the PMM-powder. Two linear motors were employed to generate moving path. A piece of 6061 Aluminum alloy plate, paved with sticky epoxy resin, was fixed on the linear motor to follow the generated path. The idea of this experiment is to use the sticky epoxy resin layer to collect the pre-mixed 4047 Al and Cu powders spraying out from the nozzle. The optical microscopy was used to observe the PMM-powder adhered on epoxy resin layer. The time of spraying powder was 25 s. During this time range, powder feeder nozzle was moving above the epoxy resin layer following the specified path "M". After the epoxy resin was solidified, the collected PMM-powder was contained in it to form the particle pattern, then for the further observation.

Table.1. Sieve analysis of pure Cu powder

Sieve type	70 mesh	100 mesh	120 mesh	140 mesh	200 mesh	325 mesh
Size (μm)	>212	150-212	125-150	106-125	75-106	45-75
Percentage (%)	0.0	1.3	2.4	3.7	47.4	45.2

Table.2. Sieve analysis of 4047 Al powder

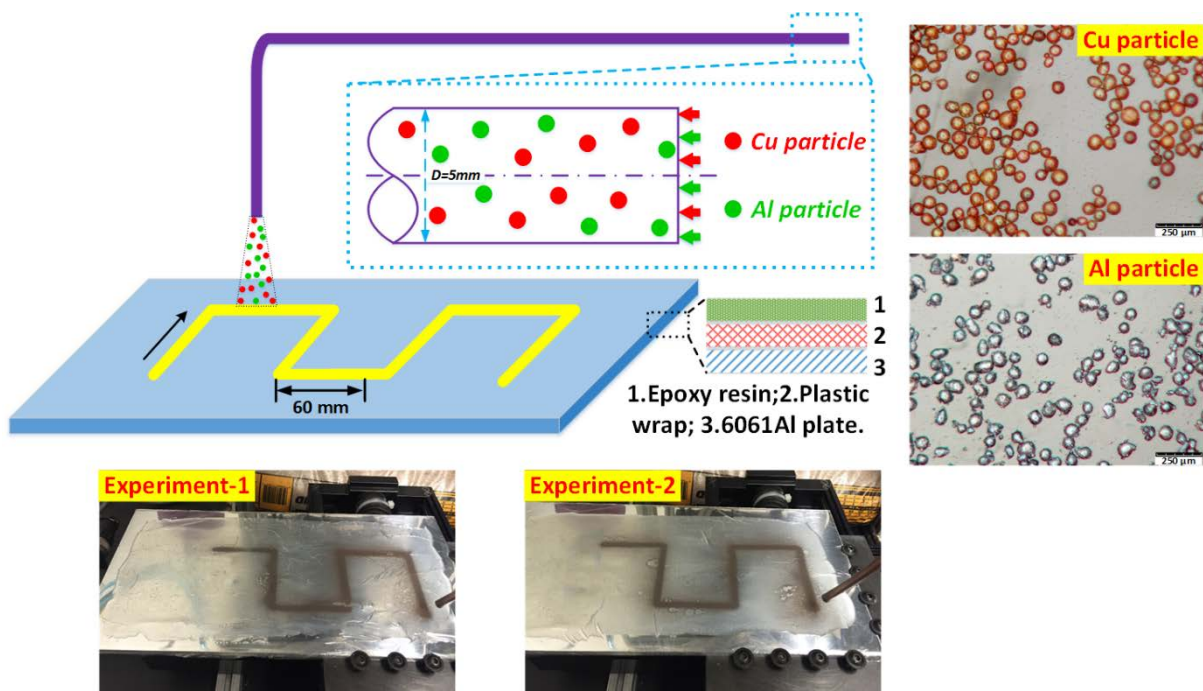| Sieve type	70 mesh	100 mesh	120 mesh	140 mesh	200 mesh	325 mesh
Size (μm)	>212	150-212	125-150	106-125	75-106	45-75
Percentage (%)	1.1	2.8	5.4	20.3	42.5	27.9

2.2. Experiment design idea

This research included two experiments. The experiment design idea was based on the thinking of particle acceleration equation in Eqn.2, which is a classic first order differential equation with variable of particle velocity u_p. The second term on the right side can be simplified as gravitational acceleration g because particle density ρ_p is much greater than argon gas density ρ. The first term on the right side contains several coefficients including argon gas flow velocity u, drag coefficient C_D, argon gas density ρ, Reynolds number Re, and the product of particle diameter d_p and density ρ_p. The coefficients u, C_D, Re, and ρ are same for all the particles, but the product of density and diameter square $\rho_p d_p^2$ varies with different types of powders.

$$\frac{d\vec{x}}{dt} = u_p \tag{1}$$

$$\frac{du_p}{dt} = \frac{18\mu}{\rho_p d_p^2} \frac{C_D Re}{24} (u - u_p) + \frac{g(\rho_p - \rho)}{\rho_p} \tag{2}$$
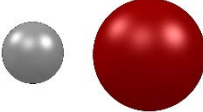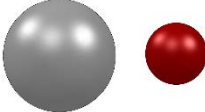
$$\rho_{p\_Cu} d_{p\_Cu}^2 = \rho_{p\_Al} d_{p\_Al}^2 \tag{3}$$

$$\frac{d_{p\_Al}}{d_{p\_Cu}} = \sqrt{\frac{\rho_{p\_Cu}}{\rho_{p\_Al}}} = \sqrt{\frac{8.94 g/cm^3}{2.6 g/cm^3}} = 1.854 \tag{4}$$

The Eqn.3 was rewritten in a new proportion format in Eqn.4, which explains an important criterion: if 4047 Al particle diameter is 1.854 times greater than Cu particle diameter, both type of particles will have same acceleration equations. Much closer the d_{p_Al}/d_{p_Cu} is to the ideal value, more effectively the PMM-powder separation could be eliminated. Otherwise, if the d_{p_Al}/d_{p_Cu} much greater or less than the ideal value, the PMM-powder will separate when flowing in powder feeder pipe since the mixed particles have different acceleration equations.

Based on above analysis, two experiments were designed. These two experiments were performed with same operating parameters, but different particle diameter. In experiment-1, the d_{p_Al}/d_{p_Cu} was much less than the ideal value. But in experiment-2, the d_{p_Al}/d_{p_Cu} is much close to the ideal value. The detailed operating parameters in the experiments were shown in Table.3.

Table.3. Sieve analysis of pure Cu powder

	Experiemnt-1	Experiment-2(optimized)
Schematic particles (Gray-Al; Red-Cu)		
4047 Al particle diameter	45-75 μm	75-106 μm
Cu particle diameter	75-106 μm	45-75 μm
d_{p_Al}/d_{p_Cu}	0.667	1.5

Vol.% ratio	50%:50%	50%:50%
Argon gas flow rate	6 m/s	6 m/s
Al plate moving speed	1m/min	1m/min
Moving time	25 s	25 s

3. Results and Discussion

3.1. Analysis methods for the experiment results

Fig. 2 shows the two solidified epoxy resin layers containing PMM-powder patterns from the two experiments. It was found that the first side in "M" shape was lost in the experiments, because when the nozzle moving along the first section of "M", the powder flow was right in the pipe. 87 observed zones with the size of 4mm by 3mm distributed with uniform-interval along the central line of the powder path for microscopic particle patterns observation. Then the distribution of different particles in the pattern was quantified. Due to the color difference of PMM-powder, the image processing software Image-J was used to mark 4047 Al particles and Cu particles in each observed zone, then count the particle numbers of two powders. Since particle sizes were known by the sieve analysis, the volume percentage of two powders in each observed zone can be calculated by Eqn.5 and Eqn.6.

$$Vol_{powder} = N_{particle} \times \frac{4}{3}\pi r_{mean}^3 \tag{5}$$

$$Vol.\%_{powder1} = 100 \times \frac{Vol_{powder1}}{Vol_{powder1} + Vol_{powder2}} \tag{6}$$
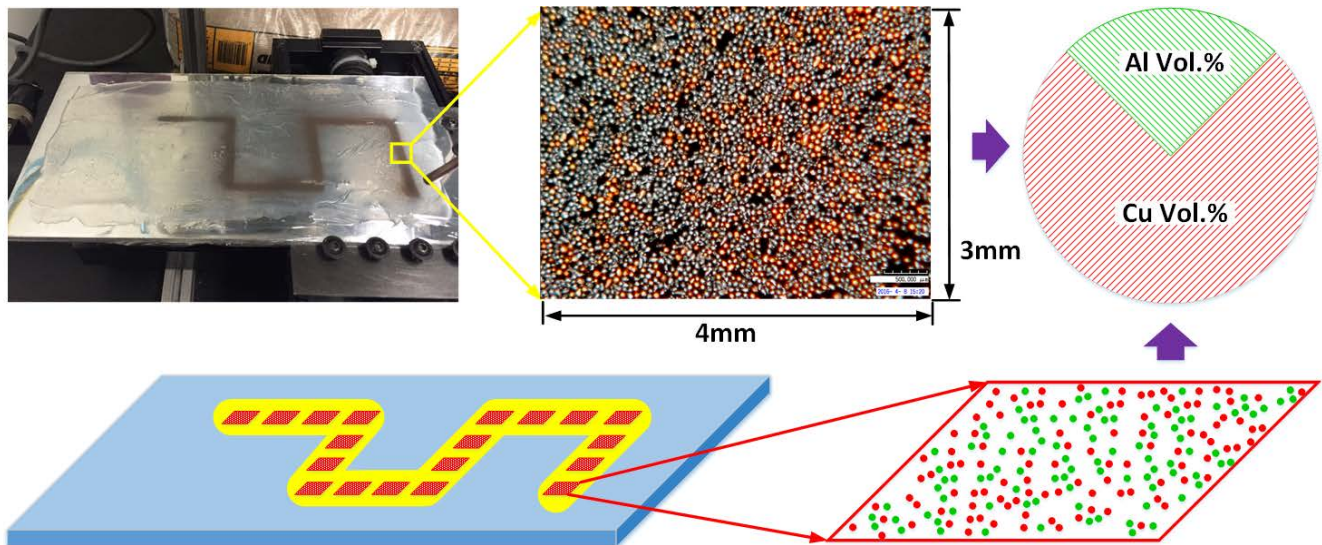

Fig.3. Observation of the experiment results.

3.2. Results of experiments

The quantification of PMM-powder patterns from experiment-1 was shown in Fig.4a. Blue color recorded the volume percentage of 4047 Al, while red color recorded the volume percentage of Cu. The time in the X-axis was used to indicate the moments when the particles in the relative observation zone reached the epoxy resin. From the PMM-powder history, a clear tendency can be found. In the beginning stage (approximately 0s ~ 4s), no particle sprayed out from the nozzle, so the volume percentage of two powders was zero. Starting from the moment of 4s, a flow of PMM-powder exited from the nozzle, in which 4047 Al was the primary particles, whose volume percentage reached to 93.25%. Some rare red Cu particles were found, whose volume percentage was 6.75%. With time increasing, more particles sprayed out from powder feeder nozzle, the primary particles are still 4047 Al, but whose volume percentage was decreasing gradually. In stark contrast, the volume percentage of Cu was gradually increasing. At the moment of 21s, Cu and 4047 Al had approximately same volume percentage. Then from the moment of 21s to the end, Cu powder volume percentage surpassed the 4047 Al powder volume percentage. Since both powders started to transit simultaneously from powder feeder pipe inlet, and 4047 Al particle had bigger acceleration than Cu particle according to the Eqn. 2, 4047 Al moved faster and exited from nozzle earlier than Cu particle. This is why Al powder volume percentage was greater than Cu powder. The powder volume percentage history in Fig.4a implied the PMM-powder separation since the two powders' volume percentage were not uniform and kept changing, although they were designed as 50%:50%. The PMM-powder separation in their flow movement ruined the powder design and resulted in the severe composition deviation between designed FGM and real deposited FGM.

The quantification of PMM-powder composition patterns in experiment-2 was shown in Fig.4b. By observing the optimized PMM-powder's composition distribution patterned in the epoxy resin coating, the PMM-powder flow had basically constant volume percentages, which were close to 50%:50%. Comparing with the results in experiment-1, the powder separation was effectively eliminated, so that the composition deviation was reduced.
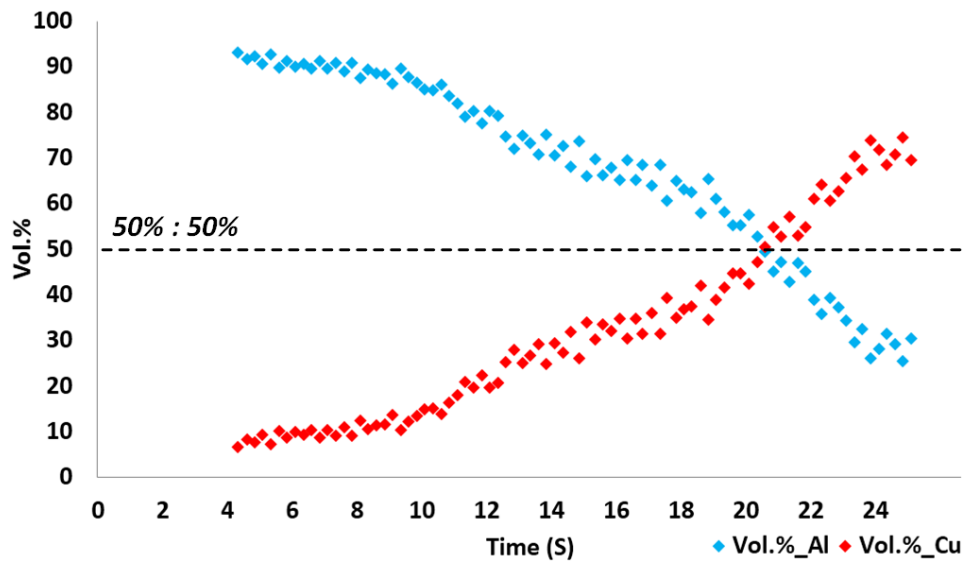
(a)
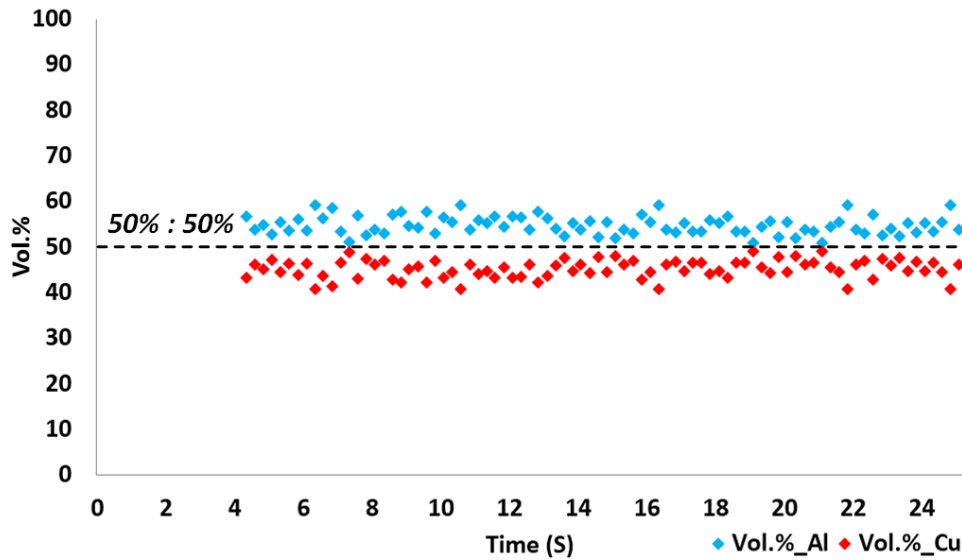
(b)

Fig.4. PMM-powder volume percentage history in (a)experiment-1, and (b)experiment-2.

4. Conclusion

Some conclusions in this paper were summarized as follows.

In the PMM-powders, which have two types of powder with different densities, if the particle diameter ratio is equal to or close to an ideal value, all the particles will have the same acceleration when moving in powder feeder pipe. The ideal value is the square root of powder density ratio. Therefore, there will be very less powder separation. The designed composition in PMM-powder can be retained.

Otherwise, if the particle diameter ratio is much greater or less than the ideal value, powder separation will happen in powder feeder pipe due to the different particle accelerations. It will cause the deviation between designed composition and real composition. The composition gradient in FGM will be ruined.

Reference

[1] Rabin, B., and Shiota, I., 1995, "Functionally Gradient Materials," MRS bulletin, 20(01), pp. 14-18.
[2] Yumin, Z., Xiaodong, H., and Jiecai, H., 1998, "Functionally Gradient Materials," Aerospace Materials & Technology, 28(5), pp. 5-10.
[3] HUANG, J.-d., WU, J., WANG, Y.-p., and HUANG, Q.-a., 2002, "Functionally Gradient Materials," Materiais Protection, 12, p. 002.
[4] Labudovic, M., Hu, D., and Kovacevic, R., 2003, "A three dimensional model for direct laser metal powder deposition and rapid prototyping," Journal of materials science, 38(1), pp. 35-49.

[5] Dinda, G., Dasgupta, A., and Mazumder, J., 2009, "Laser aided direct metal deposition of Inconel 625 superalloy: microstructural evolution and thermal stability," Materials Science and Engineering: A, 509(1), pp. 98-104.

[6] Pan, H., Sparks, T., Thakar, Y. D., and Liou, F., 2006, "The investigation of gravity-driven metal powder flow in coaxial nozzle for laser-aided direct metal deposition process," Journal of manufacturing science and engineering, 128(2), pp. 541-553.

[7] Pan, H., and Liou, F., 2005, "Numerical simulation of metallic powder flow in a coaxial nozzle for the laser aided deposition process," Journal of Materials Processing Technology, 168(2), pp. 230-244.

[8] Tan, H., Zhang, F., Wen, R., Chen, J., and Huang, W., 2012, "Experiment study of powder flow feed behavior of laser solid forming," Optics and Lasers in Engineering, 50(3), pp. 391-398.

[9] Pinkerton, A. J., and Li, L., "A verified model of the behaviour of the axial powder stream concentration from a coaxial laser cladding nozzle," Proc. Proceedings of ICALEO.

[10] Wen, S., Shin, Y., Murthy, J., and Sojka, P., 2009, "Modeling of coaxial powder flow for the laser direct deposition process," International Journal of Heat and Mass Transfer, 52(25), pp. 5867-5877.